

# Polarization Assignments in the Vacuum UV Spectra of the Primary Amide, Carboxyl, and Peptide Groups

Leigh B. Clark

Contribution from the Department of Chemistry and Biochemistry, University of California, San Diego, La Jolla, California 92093-0359

Received March 13, 1995<sup>®</sup>

**Abstract:** Polarized VUV absorption spectra of single crystals of propanamide and *N*-acetylglycine to 83 000 cm<sup>-1</sup> (120 nm) are presented. The absorption curves are obtained from the corresponding reflection spectra by Kramers–Kronig analysis. The NV<sub>1</sub> transition of propanamide appears at 53 000 cm<sup>-1</sup> (185 nm) and is polarized at -35° ± 3°. (The C–O axis is taken as the reference axis, and positive angles are measured toward the N atom of the amide group.) The second ππ\* transition appears near 78 000 cm<sup>-1</sup> (128 nm) and is polarized at +46° ± 8°. Evidence for a weaker, in-plane polarized band (amide R<sub>1</sub>) near 51 000 cm<sup>-1</sup> (196 nm) is presented. This band is in addition to the nπ\* (amide W band) which appears in solution at lower energy yet, 45 500 cm<sup>-1</sup> (220 nm). The spectrum of *N*-acetylglycine is basically a superposition of the spectra of a secondary amide (peptide) linkage and a carboxyl group. The peptide NV<sub>1</sub> band appears at 52 000 cm<sup>-1</sup> (192 nm) with a polarization direction of -55° ± 5°. A band that appears near 64 000 cm<sup>-1</sup> (156 nm) and that has no counterpart in the simple amide spectrum is assigned as the carboxyl NV<sub>1</sub>' (prime signifying local to the carboxyl) and is polarized locally at either -61° or 4° both ±3° (C–O reference axis, positive toward hydroxyl). The amide NV<sub>2</sub> band appears near 72 000 cm<sup>-1</sup> (139 nm) with a polarization of 10° or 61° both ±10°. Evidence for other, weaker bands is presented. INDO/S calculations for both systems are found to be in reasonably good agreement with the experimental results. Exciton mixing calculations suggest that crystal interactions do not lead to significant changes in apparent transition moment directions.

## Introduction

The measurement of polarized crystal spectra and the subsequent assignment of either the symmetry species of the excited configurations of symmetrical molecules or the exact directions of the transition moments of molecules with little symmetry are essential steps in the development of quantum chemical theories about the electronic structure of molecules. Such data supply important targets or goals upon which these theories are judged and advanced. In this regard, there is no transition moment direction that is not of value. In addition, knowledge of the transition moment directions for individual chromophores permits the treatment and interpretation of the various optical properties of dimers, polymers, *etc.* through additional theories that bring into play intermolecular interactions between the monomer units. The optical properties of polymers are generally sensitive to the details of conformation, and therefore the free monomer transition moment directions serve as vital parameters in the investigation of polymer conformation.

In particular, the elucidation of the structure and conformation of polypeptides and proteins through studies of optical spectra (absorption, circular and linear dichroism, *etc.*) finds its foundation in the understanding of the electronic spectrum of the basic peptide linkage (generally the secondary amide group). The needed experimental information for the basic chromophore includes the number of excited states present (in the observable wavelength range), the nature of the various transitions (*i.e.*, n → π\*, π → π\*, Rydberg), and, importantly, the transition moment vectors connecting the ground state and the various excited states. Reports of the transition moment direction of the principal amide π → π\* absorption band (called NV<sub>1</sub> in Mulliken's original notation) show differences that affect the computation and interpretation of the optical properties of

polymers. In fact, Schellman and Becktel in reviewing such data remarked, "the variations shown make a large difference to the results of optical calculations, especially optical activity".<sup>1</sup>

Transition moment directions are derived most commonly from polarized crystal spectra, and it is well-known that exciton mixing can sometimes distort the outcome. Further, as reported by Woody,<sup>2</sup> the problem is compounded because the electrostatic fields resulting from electric dipole moments of the molecules in a lattice can also modify the apparent transition moment directions derived from crystal spectra. However, in order to investigate these effects, unambiguous experimental results are needed for comparison to theoretical predictions at various levels. The apparent crystal results can be linked to the predictions of MO theoretical methods for free molecules through the theories for the distortions caused by the crystal field.

These things being so, we have reinvestigated the question of the polarization directions in amides with the aim of more firmly establishing the experimental values. The magnitudes of transition moment vectors can be found simply from the integrated area of the absorption bands, but the vector directions or polarizations require experiments with polarized light and oriented samples. Robin has reviewed all available information for the amide chromophore.<sup>3</sup> What follows is first a summary of Robin's review and then a critique of the existing evidence for the polarization assignment of the principal amide band, NV<sub>1</sub>. This critique serves as the basis for the experiments reported in this paper.

In the vapor state amides appear to exhibit a five-band pattern (W, R<sub>1</sub>, NV<sub>1</sub>, R<sub>2</sub>, and Q). This five-band pattern reduces in

(1) Schellman, J. A.; Becktel, W. J. *Biopolymers* 1983, 22, 171.

(2) Woody, R. W. *Federation of the European Chemical Society International Conference on Circular Dichroism*; Sofia, Bulgaria, Conference Proceeding 6, 1985; p 270.

(3) Robin, M. B. *Higher Excited States of Polyatomic Molecules*; Academic Press: Orlando, FL, 1975; Vol. II.

<sup>®</sup> Abstract published in *Advance ACS Abstracts*, July 1, 1995.

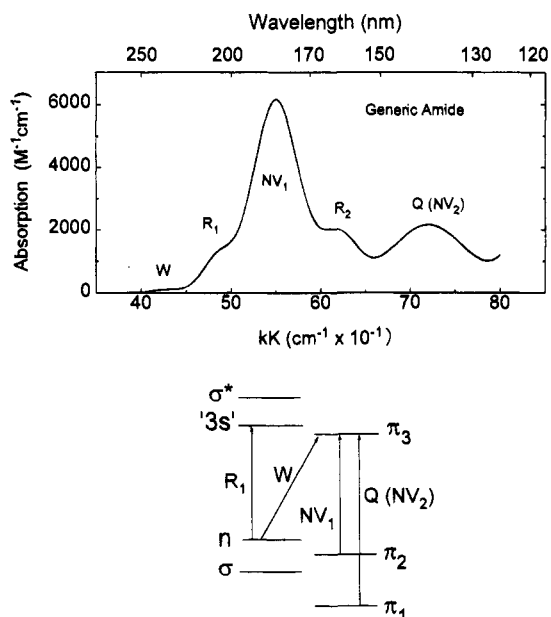


**Figure 1.** (Upper) Generic amide vapor absorption spectrum. This spectrum is a general composite of various amide spectra given by Robin. This spectrum was constructed using an oscillator strength of 0.17 for the  $NV_1$  band. Following Robin, we serially label the  $\sigma$  orbitals as  $\pi_1$ ,  $\pi_2$ , and  $\pi_3$ . Many previous workers have labeled these orbitals as  $\pi_+$ ,  $\pi_0$ , and  $\pi_-$ , respectively. (Lower) A schematic energy level diagram for pertinent valence shell orbitals. Presumed transitions are shown as arrows. The  $R_1$  and  $R_2$  bands have been assigned as Rydberg transitions.

condensed phases (solution or solid film) to an apparent two-band pattern. A weak  $n \rightarrow \pi^*$  transition is always assumed to be also present in the red edge of the absorption onset, and therefore the condensed phase pattern really involves at least three transitions. Figure 1 shows a schematic of the five-band gaseous amide pattern. The assignment of transitions according to the orbital energy diagram is also shown (four  $\pi$  electrons on three centers). According to Robin,<sup>3</sup> the  $R_1$  and  $R_2$  bands are Rydberg transitions involving big orbit, excited state functions because they seem to disappear upon going to a condensed phase. All agree that the weak, lowest energy  $W$  band is the  $n \rightarrow \pi_3^*$  transition and that the principal band near 185 nm is the  $NV_1$  transition (or  $\pi_2 \rightarrow \pi_3^*$ ). There is little evidence for the assignment of the  $Q$  band. This absorption has been variously assigned as  $\pi_1 \rightarrow \pi_3^*$  (*viz.*  $NV_2$ ) and/or as  $n \rightarrow \sigma^*$  based on theoretical calculations. After all, what else is there?

Upon going to a condensed phase the  $NV_1$  shifts to lower energy by 2 to 5 kK (kK = kiloKaiser =  $10^3 \text{ cm}^{-1}$ ), while the  $W$  band shifts to higher energy. And, according to Robin, the  $R_1$  band is *squeezed* out of existence owing to its Rydberg nature.<sup>4</sup> On the other hand, a more or less unexplained feature has been occasionally observed at about 48 kK (210 nm) in various polyamino acid spectra.<sup>5,6</sup>

In this paper we will report polarized crystal spectra taken from single crystals of propanamide and *N*-acetylglucine (Figure 2) that are aimed at more firmly establishing the polarization direction of the  $NV_1$  band of both primary and secondary amides. In addition, evidence for the polarization of bands originating within the carboxyl group is obtained in the process. First, it is useful to critique prior experiments in this area. There

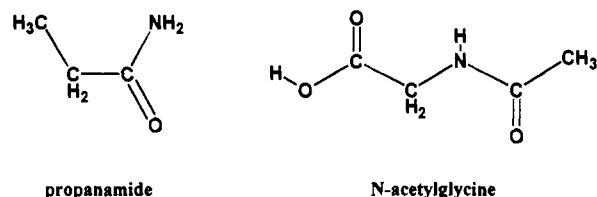


**Figure 2.** Structures of propanamide and *N*-acetylglucine.

have been but three studies employing polarized light and crystals with regard to the amide or peptide linkage and none to our knowledge with regard to the carboxyl group. The amide absorption edge appears in the vicinity of 240 nm, and the first absorption maximum occurs at about 185 nm. Polarized vacuum UV experiments on crystal specimens are thus necessary, and this requirement apparently has impeded past investigation in this regard.

The first polarization evidence for amides was published about 40 years ago by Ward.<sup>7</sup> Thin crystals of *N*-acetylglucine were grown between quartz plates, and the *bc* crystal face was identified as being parallel to the plates. This face is the normal cleavage plane and is parallel to the molecular planes. Ward's crystal specimens were too thick to transmit below about 210 nm; nevertheless the dichroic ratio *c:b* at 210 nm was found to be "certainly higher than 20:1 and may have been as high as 60:1". Since the C-N bond of the amide linkage lies about  $4^\circ$  from the *c* crystal axis, Ward concluded that the transition moment direction of the  $NV_1$  band (assumed to be in the plane of the amide linkage) must lie within  $10^\circ$  or so of the C-N line. [Actually the 20:1 ratio gives a value of  $17^\circ$ , and the 60:1 ratio corresponds to  $11^\circ$ .] Since the dichroic ratio reported by Ward was measured at the red edge of the absorption that leads to the maximum near 185 nm, one must be concerned that the reported value might not be purely representative of the  $NV_1$  band. In fact it may represent some other transition.

In 1957 Peterson and Simpson<sup>8</sup> published their well-known paper on the polarized crystal spectra of the *ab* face of myristamide [tetradecanamide,  $\text{NH}_2\text{CO}(\text{CH}_2)_{12}\text{CH}_3$ ]. The sublimation flakes that they used were thin enough to obtain transmission data to below 170 nm except for the most strongly absorbing portion of the *a* axis spectrum. They extrapolated the peak of the *a* axis band at about 187 nm in a reasonable fashion and then took the dichroic ratio, (*a:b*) = 14.6, of the red half of the band to be representative of the  $NV_1$  band. This procedure was done to avoid the blue end of the band region where a distinct peak appeared at about 178 nm along the *b* crystal axis and where the dichroic ratio dropped below unity. In any event, the value of 14.6 was shown to be consistent with the two in-plane polarization directions  $9.1^\circ$  and  $26.7^\circ$  from the N-O line toward the C-N line or C-O line, respectively.

Peterson and Simpson selected the  $9.1^\circ$  value based on two arguments. If Ward's dichroic ratio at 210 nm for *N*-acetylglucine was, in fact, representative of the strong amide  $NV_1$  band, then the requirement of mutual consistency would clearly rule out the  $26.7^\circ$  choice in myristamide. Second, they measured the direction of the principal axis of crystalline *N,N'*-diacetylhexamethylenediamine grown from the melt between quartz plates. From morphologic features they concluded that the crystal plane parallel to the quartz plates was the *bc* face of this triclinic system. The angle that the principal absorption axis (at 210 nm) made with the *c* axis was deduced to be consistent only with the  $9.1^\circ$  choice. Unfortunately, some of the atomic coordinates originally published in the crystal structure of this compound have been subsequently shown to

(4) Basch, H.; Robin, M. B.; Kuebler, N. A. *J. Chem. Phys.* **1967**, *47*, 1201.

(5) Bensing, J. L.; Pysh, E. S. *Macromolecules* **1971**, *4*, 659.

(6) Momii, R. K.; Urry, D. W. *Macromolecules* **1968**, *1*, 373.

(7) Ward, J. C. *Proc. Roy. Soc. (London)* **1955**, A228, 205.

(8) Peterson, D. L.; Simpson, W. T. *J. Am. Chem. Soc.* **1957**, *79*, 2375.

be in error (see Appendix), and the result of these errors is to invalidate the argument presented by Peterson and Simpson. Either the crystal face they used was other than the *bc* face or the axes were somehow misidentified.

Nevertheless, if Ward's dichroic ratio is even roughly representative of the  $NV_1$  in *N*-acetyl glycine, then the 9.1° choice for myristamide is correct. If, on the other hand, it is not representative of the  $NV_1$  band, then the choice cannot be made. Further, since the angular values obtained for myristamide are dependent on the dichroic ratio used, the final result is made fuzzy owing to the variation in the dichroic ratio across the band envelope.

The final crystal experiment was carried out on diketopiperazine by Kaya and Nagakura.<sup>9</sup> Here, absorption spectra to about 165 nm were measured for the (010) face of this cyclic dipeptide. The molecules project almost edge on for this face, and the presumed dimer-split  $NV_1$  transition moment direction of  $\sim 9^\circ$  is almost perpendicular to the face. Spectra were taken polarized parallel and perpendicular to the projection of the molecular planes onto (010). The observed bands were interpreted as representative of other transitions and not  $NV_1$ . All in-plane polarized transitions project with more or less intensity in the parallel direction and are therefore distinguishable from bands polarized normal to the molecular plane. Kaya and Nagakura found a weak band (the A band) near 200 nm polarized in the perpendicular direction and a stronger band (B band) near 187 nm in the parallel (in-plane) direction. They assigned the A band as the  $n \rightarrow \pi^*$  transition, and then using intensity arguments they assigned the B band to an  $n \rightarrow \sigma^*$  transition. It was presumed that owing to the dimer interaction the  $NV_1$  band was shifted to higher energy yet and therefore fell beyond their low wavelength limit of about 165 nm. No conclusion was therefore drawn regarding the polarization of the principal peptide band,  $NV_1$ .

The only value for the polarization of the  $NV_1$  band of any amide derived from direct evidence is that one obtained for myristamide by Peterson and Simpson. In spite of the above mentioned vague uncertainties their value has been assumed in virtually all the many calculations of the optical properties of chiral amides, polypeptides, and proteins.<sup>1,2,10</sup>

Given the uncertainties discussed above, it was felt worthwhile to reinvestigate the polarization direction of the  $NV_1$  band of amides with modern reflectance techniques. Our aim is to remove the lingering doubts and lurking suspicions and to establish more firmly this transition moment direction. To this end we have collected polarized reflectance data from crystals of both propanamide and *N*-acetyl glycine. Corresponding absorption curves have been obtained by Kramers-Kronig analysis, and the resulting spectra have been interpreted so as to obtain the polarization direction of the  $NV_1$  and  $NV_2$  bands of both the primary amide group (propanamide) and the peptide linkage (*N*-acetyl glycine). Furthermore, a transition occurs in *N*-acetyl glycine that is not observed in propanamide but is attributed to the  $NV_1$  transition of the carboxyl group. Evidence is presented for the possible presence of the  $R_1$  band for both the amide and the carboxyl groups in the crystal.

### Apparatus

The basic vacuum UV reflection microspectrophotometer has been described before.<sup>11,12</sup> For the present work a significant modification has been made, and that change will be discussed

here. The magnesium fluoride polarizer has now been removed. In past work a  $MgF_2$  Rochon polarizer set to employ only the horizontally polarized beam was used. The resulting polarized beam was incident upon a 45° beam splitter (double LiF plates). The design of the instrument is such that radiation going toward the crystal is transmitted through the beam splitter, and upon reflecting from the crystal surface a fraction of the beam experiences a reflection upwards from the beam splitter toward the detector. In practice the portion of the incident beam initially deflected downward by the beam splitter is reflected from a standard LiF reflector plate back through the beam splitter to the detector. The two channels are chopped at different individual frequencies and are detected simultaneously by the photomultiplier tube. The two signals are extracted from their composite by two lock-in amplifiers tuned to the individual chopping frequencies, and their ratio is recorded by a laboratory computer. In order to arrive at a crystal reflection spectrum (say polarized along a particular optical axis of some face), two scans are required. First the crystal is oriented at normal incidence with the optical axis of interest aligned parallel to the polarization of the radiation (horizontal), and the ratio of both channels is scanned. Next the crystal is replaced with a standard LiF reflector, and new ratio of both channels is scanned. The absolute reflection spectrum is then obtained as

$$R = \frac{\text{ratio}^{\text{xtal}}}{\text{ratio}_{\text{LiF}}} R_{\text{LiF}}$$

where  $R_{\text{LiF}}$  is the reflectivity of LiF calculated from the index of refraction of LiF as a function of wavelength (see Appendix).

The  $MgF_2$  Rochon ( $\sim 6$  cm long) attenuated the beam severely below 150 nm so that the practical wavelength limit for measurements was in the 140–145 nm range. However, it was known that the 45° angle that the beam splitter made to the incident beam by itself caused a partial polarization to occur in the beams of both channels because 45° is not far removed from Brewster's angle. At Brewster's angle (56.3° for LiF at 150 nm) the beams arriving at the detector would be 100% polarized perpendicular to the plane of incidence of the beam splitter (i.e., horizontal) since the other polarization will then experience zero reflection at the splitter. At 45° a LiF plate provides about 90% polarization of the beam in the direction perpendicular to the plane of incidence of the splitter.

The data presented in this paper were obtained by replacing the  $MgF_2$  polarizer with a simple  $MgF_2$  window for which the optical axes were aligned at 45° relative to the plane of incidence of the beam splitter. This plate serves as a depolarizer of the radiation coming from the monochromator and insures that the incident intensity of both perpendicular (horizontal) and parallel (vertical) beam components are equivalent at the outset for every wavelength.

If the fractional polarizations created by one reflection plus one transmission at the beam splitter are  $f_\perp$  and  $f_\parallel$ , then the reflection spectra,  $R_1$  and  $R_2$ , obtained from a crystal whose *A* axis and then (subsequently) whose *B* axis are aligned horizontally will be given by expressions of the form

$$R_1 = f_\perp R_A + f_\parallel R_B \quad (1)$$

$$R_2 = f_\perp R_B + f_\parallel R_A$$

Expressions for  $f_\perp$  and  $f_\parallel$  can be obtained by noting that if the reflection and transmission coefficients for say perpendicularly polarized light at the beam splitter are  $R_\perp$  and  $T_\perp$ , then the effect of the beam splitter on an incident beam of perpendicular

(9) Kaya, K.; Nagakura, S. *J. Mol. Spec.* **1972**, *44*, 279.

(10) Woody, R. W. *J. Polymer Sci.* **1977**, *12*, 181.

(11) Zaloudek, F.; Novros, J. S.; Clark, L. B. *J. Am. Chem. Soc.* **1985**, *107*, 7344.

(12) Campbell, B. F.; Clark, L. B. *J. Am. Chem. Soc.* **1989**, *111*, 8131.

polarized light of  $I_0$  intensity is  $I_0 \mathbf{R}_\perp \cdot \mathbf{T}_\perp$ . Thus we obtain

$$f_\perp = \frac{\mathbf{R}_\perp \mathbf{T}_\perp}{\mathbf{R}_\perp \mathbf{T}_\perp + \mathbf{R}_\parallel \mathbf{T}_\parallel}$$

From the index of refraction of LiF at any wavelength the values of  $\mathbf{R}$  and  $\mathbf{T}$  for a double plate beam splitter for either polarization may be calculated. For a single LiF/vacuum boundary the reflection and transmission coefficients are given by the Fresnel relations

$$r_\parallel = \left[ \frac{\tan(\phi - \phi')}{\tan(\phi + \phi')} \right]^2 \quad r_\perp = \left[ \frac{\sin(\phi - \phi')}{\sin(\phi + \phi')} \right]^2 \quad (2)$$

$$t_\parallel = (1.0 - r_\parallel) \quad t_\perp = (1.0 - r_\perp)$$

where  $\phi$  is the angle of incidence (in our case  $45^\circ$ ) and  $\phi'$  is the angle of refraction. The angle  $\phi'$  can be evaluated from Snell's law for any given  $n_{\text{LiF}}$  and  $\phi$  as

$$\phi' = \frac{\arcsin(\phi)}{n_{\text{LiF}}}$$

For a single LiF plate with two parallel reflecting surfaces the overall transmission and reflection coefficients for each polarization are given by

$$T = r^2(1.0 + r^2 + r^4 + \dots) \quad (3)$$

$$R = (1 - T)$$

where  $r$  and  $t$  are from eq 2. These relations can be obtained by considering the multiple paths available.

Finally, a two plate beam splitter can be treated as a two "boundary" one in which each "boundary" has values  $T$  and  $R$ . Thus, taking eq 3 to the next level, we obtain

$$\mathbf{T} = T^2(1 + R^2 + R^4 + \dots)$$

$$\mathbf{R} = (1 - \mathbf{T})$$

From the index of refraction of LiF (see the Appendix) values for  $\mathbf{T}$  and  $\mathbf{R}$  for the two plate beam splitter (at  $45^\circ$ ) can be evaluated at each wavelength for both perpendicular and parallel polarization, and these values lead to the fractions  $f_\perp$  and  $f_\parallel$  in eq 1. A two plate splitter is used because it provides enhanced signal strength compared with a one plate splitter.

Given the measured values of  $R_1$  and  $R_2$  at each wavelength one can solve the two simultaneous eq 1 at each wavelength for the correct reflectivities  $R_A$  and  $R_B$ . The present results were obtained using this sort of analysis. The elimination of the  $\text{MgF}_2$  polarizer has permitted the wavelength range to be extended to 120 nm ( $83\,000\text{ cm}^{-1}$ ) although the signal-to-noise ratio decreases substantially below 150 nm owing to diminishing output from the  $\text{D}_2$  lamp. The reflectivity data were consequently smoothed in the shorter wavelength region.

The reflection spectra obtained with the above recipe were transformed to their corresponding absorption curves through Kramers-Kronig analysis.<sup>11</sup> These procedures have been described previously. Finally, transmission spectra were obtained using a nitrogen flushed, Olis-modified Cary 15 spectrophotometer. Trimethylphosphate (Aldrich) was used as the solvent for the solution spectra owing to its transparency ( $\sim 165$

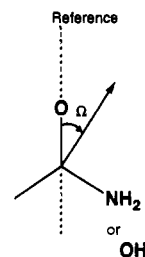


**Figure 3.** Transition moment direction convention for amide and carboxyl transitions. The positive direction of  $\Omega$  is toward the amino (or hydroxyl) group.

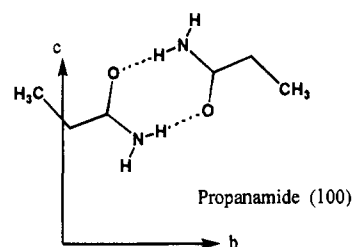


**Figure 4.** Projection of two molecules of the unit cell onto the  $bc$  face of propanamide. The molecules occur as hydrogen bonded pairs as shown. The relative disposition of the other two molecules in the unit cell can be obtained by a reflection across the  $c$  axis or the  $b$  axis. All sites are spectroscopically equivalent.

nm) and its good solvent ability. Cell pathlengths ranged from 0.01 mm up.

### Transition Moment Convention

In the earlier work on myristamide the reference axis from which the amide polarizations were given was chosen as the N-O axis.<sup>8</sup> This direction was chosen presumably because of the theoretical connection with the carboxylate or allyl anions. In our opinion this reference axis is somewhat awkward to use in practice, and a new convention is proposed in which the reference axis is chosen as the carbonyl C-O bond direction. Since the local geometry is essentially planar, the amide transitions will be polarized close to parallel or perpendicular with respect to this plane. In-plane polarized transitions are, therefore, defined by the angle  $\Omega$  they make with respect to the reference axis (positive toward the N atom in amide and the hydroxyl group in carboxyl) (see Figure 3). With this new reference axis the value of  $9.1^\circ$  given by Peterson and Simpson<sup>8</sup> for myristamide translates to  $-41^\circ$ . The C-N bond direction has also been used as a reference axis. Although the choice is arbitrary, the C-O bond reference axis has an appealing simplicity since no other atom or groups can be attached to at least one of the atoms defining the reference axis.

### Propanamide

Propanamide was selected for study because it is a simple primary amide with known crystal structure,<sup>13</sup> and it has a reasonably short alkyl chain associated with it. The amide chromophore is therefore fairly concentrated in the crystal, and this feature enhances the throw of the reflection spectra. The material is slightly volatile, however, and so the published crystal structure was determined at 123 K. The differences in unit cell dimensions between room temperature and 123 K average about 1% and have been ignored in the present study. We will assume the 123 K structure is adequate for interpretation of the room temperature spectra reported here.

The crystals were grown by placing a closed jar containing propanamide near the warm vent of a laboratory oven. Large, very thin crystal sheets formed overnight. The sheets showed

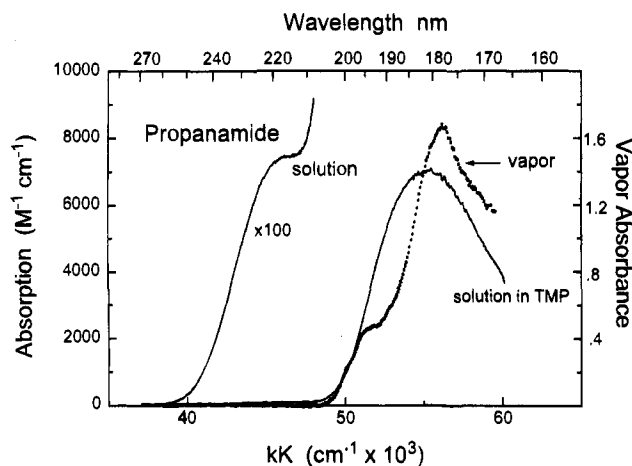


**Figure 5.** Absorption spectrum of propanamide dissolved in trimethylphosphate solvent. The vapor spectrum of propanamide near 60 °C in a 10 cm cell is also shown.

**Table 1.** Solution Spectral Data

|                         |                 | $f^a$ | $\nu$ (kK) | $\lambda$ (nm) |
|-------------------------|-----------------|-------|------------|----------------|
| propanamide             | W ( $n\pi^*$ )  | 0.002 | 46         | 220            |
|                         | NV <sub>1</sub> | 0.17  | 55.6       | 180            |
| <i>N</i> -acetylglucine | W ( $n\pi^*$ )  | 0.003 | 47         | 213            |
|                         | NV <sub>1</sub> | 0.17  | 54.1       | 185            |

<sup>a</sup> Three-dimensional oscillator strength.

uniform extinction, and some of the crystals had clearly defined boundaries. The crystal sheets are tough and can be sharply bent by 180° without fracturing. From the angles made by the edges it was deduced that the crystals were elongated along *c* and that the large face was (100). Figure 4 shows a projection of the molecules onto the (100) face. The molecules appear as hydrogen bonded dimers.

The solution spectrum of propanamide dissolved in trimethylphosphate is shown in Figure 5, and values for absorption parameters are given in Table 1. Two absorption bands are apparent: the weak W band ( $n \rightarrow \pi_3^*$ ) near 48 kK (220 nm),  $f = 0.003$ , and what is presumably the NV<sub>1</sub> band near 53 kK (187 nm),  $f = 0.17$ . If the conventional wisdom regarding the amide spectrum is correct, we should expect the crystal reflection spectra to be dominated by the NV<sub>1</sub> transition and that the W band may or may not be observed owing to its inherent weakness. We further anticipate that the R bands will have vanished in the solid phase and that the second prominent transition will be the Q band appearing at higher energy (> 70 kK). Not all of these expectations are fulfilled.

**Crystal Spectra and the NV Transitions.** Reflection spectra polarized along the *b* and *c* axes of (100) are given in Figure 6. Corresponding absorption spectra curves obtained through Kramers–Kronig analysis are shown in Figure 7. It is clear that the propanamide spectrum to about 70 kK is dominated by absorption that projects most strongly along the *c* axis and peaks near 54 kK. The *b* axis spectrum however shows a modest maximum at somewhat higher energy near 57 kK. These spectra closely resemble those obtained for the (001) face of myristamide by Peterson and Simpson.<sup>8</sup> If we assume that the main absorption in the 50–65 kK region arises from the  $\pi_2 \rightarrow \pi_3^*$  (NV<sub>1</sub>) transition and not worry about differences in peak position and band shapes between *b* and *c* and the possible presence of other transitions, then the dichroic ratio,  $f_c/f_b$ , obtained from the integrated areas under the entire band envelopes is 6.4. This ratio is consistent with two in-plane vectors directed at  $-37^\circ$  and  $+15^\circ$ . The values obtained for myristamide by Peterson and Simpson (converted to the new

angular convention) are  $-41^\circ$  and  $-7^\circ$ . The nearness of  $-37^\circ$  and  $-41^\circ$  strongly supports the choice Peterson and Simpson in fact made. It should be pointed out that the dichroic ratio upon which their result was based was taken as 14.6 (*i.e.*, from the red half of the band). If integrated band areas had been used, then their dichroic ratio would have been about 10 to 11, and the corresponding transition moment direction would have been  $-44^\circ$  or  $-4^\circ$ . As will be seen later when the spectra of *N*-acetylglucine are considered, the negative value for propanamide is most certainly the proper choice. An angle of  $-37^\circ$  is  $6^\circ$  from the N to O line tipped toward the N–C line.

Intermolecular interactions in the crystal lead to energy differences for the components of any given transition along different axes of a crystal face (Davydov splitting) and intensity borrowing among band components. This borrowing varies from axis to axis, and therefore apparent transition moment directions can be different from their free molecule values. For both propanamide and myristamide the spectra appear to be dominated by a single strong band. This situation suggests that intensity borrowing to and from bands of other polarization will have a minimal effect on the strong band and that the observed dichroic ratio will reflect the true nature of the NV<sub>1</sub> band polarization. Borrowing among the vibronic components of the single transition will however occur at will, and band shapes can therefore become distorted.<sup>14,15</sup> The dichroic ratio can therefore vary considerably over the band envelope. The use of integrated areas under band envelopes ought to yield the most representative dichroic ratio.

The calculation of crystal spectra from a single molecule model spectrum is reasonably well established.<sup>16,17</sup> We have carried through such calculations for both propanamide and myristamide. The dipole–dipole lattice sums for these calculations are given in the Appendix. For propanamide the Davydov splitting, assuming a single concentrated transition (strong coupling), is almost identical to the energy difference in band maxima obtained by breaking up the band symmetrically into a series of vibronic components (weak coupling) and carrying through a similar calculation. Entirely similar results are obtained for myristamide except that the *a* axis replaces the *c* axis as the carrier of the dominant transition component. The feature near 57 kK along the *b* axis of both crystal systems is most certainly the “Davydov shifted” component of the NV<sub>1</sub> band and not some new transition. Assuming strong coupling the Davydov splitting ( $E_b - E_c$ ) is computed to be  $3500 \text{ cm}^{-1}$ , and this value compares with the observed value of  $\sim 4000 \text{ cm}^{-1}$ .

The broad absorption in the 75–80 kK region is the only other obvious feature of the two spectra. This position is near that expected for the amide Q band (NV<sub>2</sub>). If the absorption in the 75–80 kK region is assumed to arise from a single, in-plane polarized transition, then that transition will have an oscillator strength near 0.1 and approximate direction possibilities of  $+46^\circ$  or  $-72^\circ$  (both  $\pm 8^\circ$ ).

**Other Transitions?** Several questions remain. For example, where is the  $n \rightarrow \pi^*$  transition in the crystal spectra, and what is the origin of the distinct shoulder observed in the *c* axis reflection spectrum near 50 kK? No distinct feature attributable to a weak  $n \rightarrow \pi^*$  band can be discerned in the reflection spectra, but the onset of absorption in the crystal can be seen as a decline of the “double-reflection” (observed in the transparent region of these thin crystals) that begins near 42 kK (240 nm) and is

(13) Usanmaz, A.; Adler, G. *Acta Crystallogr.* **1982**, B38, 660.

(14) Clark, L. B. *J. Am. Chem. Soc.* **1986**, 108, 5109.

(15) Xu, S.; Clark, L. B. *J. Am. Chem. Soc.* **1995**, 117, 4379.

(16) Clark, L. B.; Philpott, M. R. *J. Chem. Phys.* **1970**, 55, 3790.

(17) Craig, D. P.; Walmsley, S. H. *Excitons in Molecular Crystals: Theory and Applications*; W. A. Benjamin, Inc.: New York, 1968.

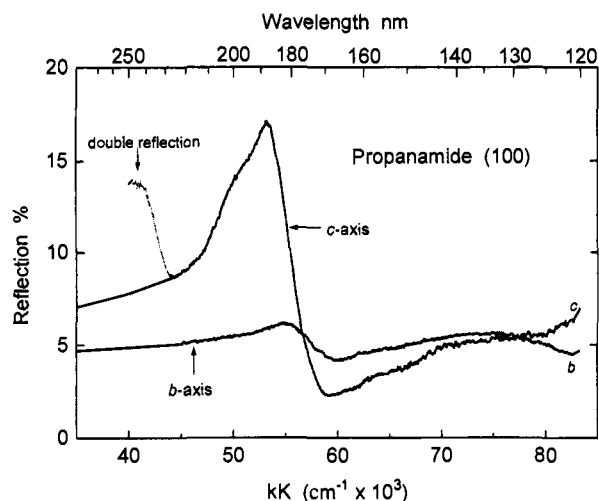


**Figure 6.** Propanamide reflection spectra polarized along the *b* and *c* axes of (100) crystal face. The curves have been smoothed below about 170 nm. Reflections from the back surface of these thin crystals contributes to the signal in the transparent region (shown for the *c* axis). The reflection spectra in the low energy region were prepared for Kramers–Kronig transformation by smoothly extending the experimental curves as shown.

complete by 44.4 kK (225 nm) [see Figure 6 for an example]. In an attempt to locate a weak  $n \rightarrow \pi^*$  band near the absorption onset, a thin crystal flake of propanamide was mounted over a pinhole and (along with calcite polarizers) was placed in the Cary spectrophotometer. After the crystal thickness was allowed to thin gradually by sublimation the absorption spectra polarized parallel to the *b* and *c* axes were examined to the calcite limit (210 nm). As expected absorption begins near 42 kK (240 nm) along both axes and is strongest along *c*. No distinct peak or even shoulder appears along either axis. The dichroic ratio (*c/b*) is about 3. The natural polarization of the amide  $n \rightarrow \pi^*$  transition is normal to the amide plane, and such a band ought to show very little projection onto the *c* axis. The relative projections *a:b:c* are 53:41:1. Clearly the experimental dichroic ratio is not consonant with that expected for the natural polarization of an  $n \rightarrow \pi^*$  band. Herzberg–Teller mixing from the nearby, strong  $\pi_2 \rightarrow \pi_3^*$  band no doubt swamps the natural  $n \rightarrow \pi^*$  polarization and produces the observed intermediate dichroic ratio (*i.e.*, between  $n \rightarrow \pi_3^*$  and  $\pi_2 \rightarrow \pi_3^*$ ). Although the W band cannot be observed in the crystal as a distinct band, it is clearly present in the solution spectrum near 45 kK (220 nm).

The shoulder near 50 kK in the reflection spectrum along the *c* axis suggests the presence of yet another transition. This shoulder is in the vicinity of spectral features observed in the crystal spectra of diketopiperazine<sup>9</sup> and some polyamino acid spectra.<sup>5,6</sup> The position is near that of the amide vapor  $R_1$  band. Further, the weak, low-energy tail in this vicinity in the *b* axis absorption spectrum supports this notion. Transformation to absorption mutes the prominence of this feature along *c*, but it can still be vaguely discerned. We have therefore attempted to resolve the spectra with the supposition that an additional transition is present near 51 kK (see Figure 7). There is considerable latitude for the *c* axis component, but, however it is done, the dichroic ratio closely resembles that for the principal transition  $NV_1$  ( $\pi_2 \rightarrow \pi_3^*$ ). If such a transition is included in the exciton mixing calculations a strong transfer of intensity is predicted to occur from  $\pi_2 \rightarrow \pi_3^*$  along the *c* axis. We have probed the calculational space for this scenario and have found that the presence of a fairly weak third transition can account for the observed feature. In fact, the resolutions shown in Figure

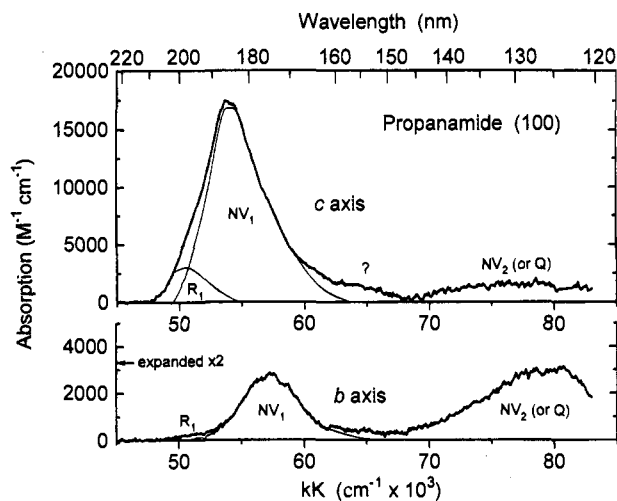


**Figure 7.** Absorption spectra of the (100) face of propanamide obtained by Kramers–Kronig analysis of the corresponding reflection spectra. The resolution of bands discussed in the text is shown as the light curves.

**Table 2.** Model Spectrum for Propanamide

|        | $f^a$ | $\nu$ (kK) | $\lambda$ (nm) | $\Omega$ (deg) <sup>b</sup> | $\Delta\Omega$ (deg) <sup>c</sup> |
|--------|-------|------------|----------------|-----------------------------|-----------------------------------|
| W      | 0.001 | 48         | 208            | $\perp$                     |                                   |
| $R_1$  | 0.01  | 51.0       | 196            | $-38$ (4)                   | $\pm 8$                           |
| $NV_1$ | 0.17  | 55.2       | 181            | $-35$                       | $\pm 3$                           |
| $NV_2$ | 0.1   | 79         | 127            | $46$ ( $-72$ )              | $\pm 8$                           |

<sup>a</sup> Three-dimensional oscillator strength. <sup>b</sup> Alternate values in parentheses are also consistent with the observed spectra; however based on the evidence they are the least likely choice. <sup>c</sup> Uncertainty estimated from experimental resolutions.

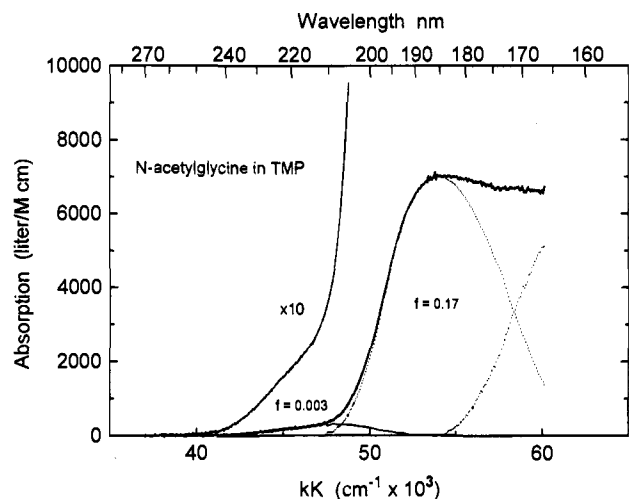
7 are consistent with a model free-molecule spectrum that includes a transition at 51 kK with an oscillator strength of 0.01 directed at either  $+4^\circ$  or  $-38^\circ$ . Since this intensity is just about the value ascribed to the general amide  $R_1$  band, we feel that Robin's assertion that it is not observed in condensed phases may need reconsideration. The absorption spectrum of propanamide vapor (60 °C) to 167 nm in a 10 cm silica cell is shown in Figure 5, and the presence of the  $R_1$  transition as a double humped band (spacing  $\sim 1280$   $\text{cm}^{-1}$ ) is apparent. We estimate the oscillator strength to be no larger than one-tenth that of the  $NV_1$  band. The  $NV_1$  band shifts to lower energy upon going to a condensed phase and presumably obscures the  $R_1$  band in both the crystal and solution absorption spectra. Since reflectivity has a derivative-like component, the visibility of the  $R_1$  band is enhanced in reflection.

**Summary.** A model spectrum for propanamide has been constructed using the above analysis and is given in Table 2. When this model spectrum is used as the starting point for a calculation of crystal spectra, then a reasonable fit occurs. The calculated and observed values for the oscillator strengths and energies for the various bands along the *b* and *c* axes are compared in Table 3. The results shown were obtained taking the direction of  $NV_2$  to be  $46^\circ$ , but entirely equivalent results are obtained if the alternate angle of  $72^\circ$  is employed. These calculations indicate that an apparent shift of a mere  $2^\circ$  occurs for  $NV_1$  as a result of crystal interactions ( $-35^\circ \rightarrow -37^\circ$ ). In summary, the spectra presented show evidence for four transitions (W,  $R_1$ ,  $NV_1$ , and  $NV_2$ ). Although vague features near the expected position of  $R_2$  ( $\sim 64$  kK) are observed in the crystal spectra, no conclusions can be reached regarding the presence of bands there owing to noise limitations. On the other hand, INDO/S molecular orbital calculations place some weak transitions in this vicinity (*vide infra*).

**Table 3.** Observed and Calculated Crystal Spectra of Propanamide<sup>a,b</sup>

|                 | <i>b</i> axis |              |          |              | <i>c</i> axis |              |          |              |
|-----------------|---------------|--------------|----------|--------------|---------------|--------------|----------|--------------|
|                 | calc          |              | exper    |              | calc          |              | exper    |              |
|                 | <i>f</i>      | ( <i>ν</i> ) | <i>f</i> | ( <i>ν</i> ) | <i>f</i>      | ( <i>ν</i> ) | <i>f</i> | ( <i>ν</i> ) |
| W               | 0.001         | (48.0)       | ...      | (<45)        | 0.000         | (48.0)       | ...      | (<45)        |
| R <sub>1</sub>  | 0.003         | (51.1)       | 0.003    | (~51)        | 0.06          | (50.9)       | 0.05     | (~51)        |
| NV <sub>1</sub> | 0.07          | (57.3)       | 0.07     | (57.5)       | 0.41          | (54.0)       | 0.42     | (54.0)       |
| NV <sub>2</sub> | 0.13          | (78.6)       | 0.12     | (~79)        | 0.07          | (78.9)       | 0.07     | (~78)        |

<sup>a</sup> Calculated using the model spectrum given in Table 2. Energies are given in kiloKaiser. Oscillator strengths are one-dimensional, crystal values. <sup>b</sup> An ellipsis (...) implies that this feature was not observed experimentally.

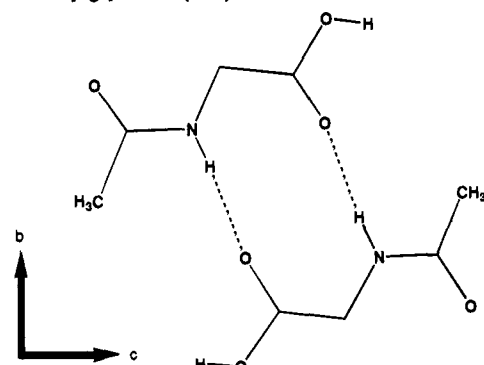
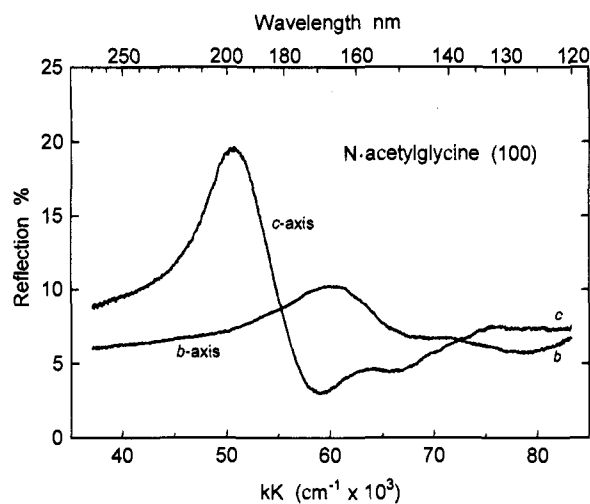
**Figure 8.** Absorption spectrum of *N*-acetylglycine dissolved in trimethylphosphate.

### *N*-Acetylglycine

*N*-Acetylglycine occurs as a neutral species in the crystal and so gives an opportunity to examine both a secondary amide group (peptide linkage) and a carboxylic acid group together in the same system. The spectrum of the carboxyl group is expected to mimic closely the spectrum of the amide group except it will be displaced somewhat to higher energy. Robin has summarized available data on carboxyl and has identified the same sequence of bands (W, R<sub>1</sub>, NV<sub>1</sub>, R<sub>2</sub>, and Q) in both systems.<sup>3</sup> For clarity, we will use a prime on carboxyl transitions in order to distinguish them from corresponding amide transitions. With the exception of the W' band, all transitions of carboxyl are shifted 5–10 kK to higher energy relative to those of amide.<sup>3</sup> The solution spectrum of *N*-acetylglycine is shown in Figure 8, and values for absorption parameters are given in Table 1. The spectrum is similar to that of propanamide in that a region of weak  $n \rightarrow \pi^*$  absorption (W/W', 46 kK,  $f \approx 0.003$ ) is followed by a stronger band (NV<sub>1</sub>, 54 kK,  $f = 0.17$ ).

Large (1 cm) crystals are easily grown from aqueous solution either by slow cooling or slow evaporation. The molecules form hydrogen bonded sheets in the crystal that are almost exactly parallel to the *bc* crystal plane.<sup>18–20</sup> The projection onto (100) is shown in Figure 9. The hydrogen bonding arrangement is quite different from the simple amide scheme (in which the amide groups pair up head-to-head in dimer-like fashion). Here molecules are paired through hydrogen bonds between the amide nitrogen of one molecule and the carbonyl oxygen of the

### *N*-acetylglycine (100)

**Figure 9.** Projection of two molecules of the unit cell of *N*-acetylglycine onto the (100) crystal face. The principal hydrogen bonds are indicated. The relative disposition of the other two molecules can be obtained by reflection of the two shown across the *c* or the *b* axes. All sites are spectroscopically equivalent.**Figure 10.** *N*-acetylglycine reflection spectra polarized along the *b* and *c* axes of the (100) crystal face. The curves have been smoothed below ~170 nm.

carboxylic acid group of adjacent molecules. The (100) face shows perfect cleavage, and the spectra reported here were taken from freshly cleaved surfaces. The reflection spectra obtained from the (100) face are shown in Figure 10, and the corresponding absorption spectra are presented in Figure 11. In addition to the strong amide NV<sub>1</sub> band near 52 kK there appear an additional absorption peak along each axis near 64 kK as well as another band principally along *b* near 72 kK. Yet another band near 78 kK may also be present. The 64 kK band presumably arises from an excitation of the carboxylic acid group since there is no corresponding absorption in the simple amide spectra.

**Peptide Transitions. a. NV<sub>1</sub> Band.** There appears to be a 2000  $\text{cm}^{-1}$  shift to the red for the NV<sub>1</sub> band going from a primary amide to the secondary amide of *N*-acetylglycine. Further, this transition projects almost entirely along the *c* crystal axis. We estimate the dichroic ratio [*c*/*b*] to exceed 200 near the peak at 51 kK. Actually, the ratio evaluated from the experimental data exceeds 1000, but the uncertainty in the calculated extinction coefficients is at least  $\pm 100$  extinction units ( $\text{L/mol}\cdot\text{cm}$ ) owing to the Kramers–Kronig transformation criteria. Interestingly, at 51 kK there is a very slight but definite minimum in the *b* axis spectrum. Thus the dichroic ratio at 210 nm is about 60, and this value is the upper limit given by Ward for his transmission measurement.<sup>7</sup> However, owing to the insensitivity of  $\cos^2 \theta$  with changing  $\theta$  near  $\theta = 0^\circ$  a dichroic

(18) Carpenter, G. B.; Donohue, J. *J. Am. Chem. Soc.* **1950**, *72*, 2315.

(19) Donohue, J.; Marsh, R. E. *Acta Crystallogr.* **1962**, *15*, 941.

(20) Mackay, M. F. *Cryst. Struct. Comm.* **1975**, *4*, 225.

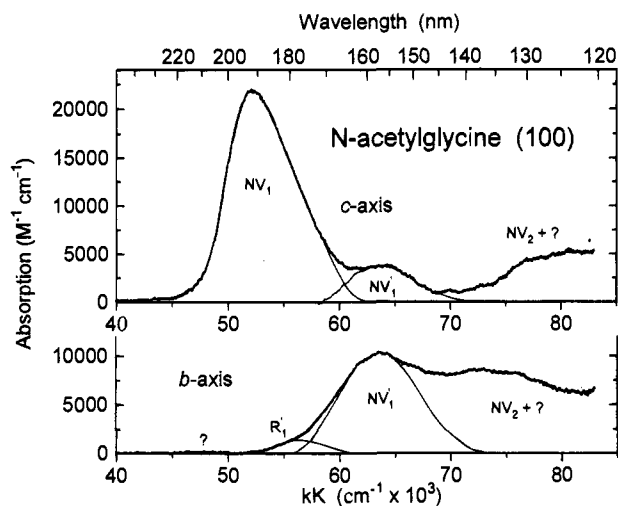


**Figure 11.** Absorption spectra of the (100) face of *N*-acetylglycine. The resolution of bands discussed in the text is shown as light curves.

ratio of even 200 translates into a substantial angular difference of  $8^\circ$ . The possible transition moment directions are then  $-59^\circ$  and  $-51^\circ$ . Since the individual vibronic components of any electronic transition can be expected to display a wobble in their directions of up to a few degrees to either side of an overall average, we choose the average value of  $-55^\circ$  for this polarization. An uncertainty of  $\pm 5^\circ$  is consistent with the possible change in the  $c/b$  dichroic ratio down to 100:1. The  $-55^\circ$  value rules in favor of the propanamide choice of  $-36^\circ$  relative to the alternate choice there of  $15^\circ$ .

**b.  $n \rightarrow \pi^*$  Transition.**  $n \rightarrow \pi^*$  absorption occurs near 220 nm in the solution spectrum with an extinction coefficient of about 150. Since the  $n \rightarrow \pi^*$  bands of both the amide and the carboxyl groups are expected in the same vicinity, the two are probably not distinguishable. The absorption edge of a thin crystal slab cleaved parallel to (100) occurs near 242 nm and shows much stronger, beginning absorption along  $b$  than along  $c$  (dichroic ratio  $b/c \approx 5$ ). This result is surprising for on the one hand the "natural", allowed polarization of such a band is normal to the amide plane and presumably cannot be observed in the  $bc$  face spectra. Only borrowed (or "forbidden") intensity can be observed polarized in the (100) crystal plane. On the other hand, the presumed mechanism for intensity borrowing is Herzberg–Teller coupling with nearby strong transitions, and the only nearby, strong band is  $NV_1$  and is polarized strictly along the  $c$  axis. The experimental results stands however.

**c.  $R_1$  Band.** No evidence for the  $R_1$  band is apparent in the crystal spectra. If an  $R_1$  band is present here as in propanamide, then it must have a polarization very near that of the  $NV_1$  band. If it were otherwise, then a component along  $b$  would be easily observed. The fact that no  $b$  axis component is apparent in *N*-acetylglycine rules in favor of the  $-38^\circ$  choice over the  $4^\circ$  choice for  $R_1$  in propanamide. If both  $R_1$  and  $NV_1$  here have about the same direction, then the red shift of the  $NV_1$  band will obscure  $R_1$  completely.

**d.  $NV_2$  Band.** Looking past the bands near 64 kK (ascribed to carboxyl), the region between 70 and 80 kK appears to be composed of at least two band systems with oscillator strengths of about 0.1. If so, then the first in the vicinity of 73 kK shows a dichroic ratio ( $b/c$ )  $\approx 5$  ( $\Omega = +10^\circ$  or  $+60^\circ$ ), and the second near 80 kK shows a dichroic ratio ( $b/c$ )  $\approx 1$  ( $\Omega = +17^\circ$  or  $+79^\circ$ ). The above direction possibilities refer to the amide origin. INDO/S computations (*vide infra*) predict this region to be complex, but that is not inconsistent with the above analysis.

**Carboxyl Transition.** The bands near 64 kK in both  $c$  and  $b$  polarization are undoubtedly derived from a transition of the carboxyl group. Randomizing the crystal spectra suggests this band would show a vapor spectrum extinction of just under 5000 ( $M \text{ cm}^{-1}$ ), and this value corresponds to that observed for what has been assigned as the  $NV_1'$  band in the vapor spectrum of trifluoroacetic acid.<sup>21</sup> Using a transition moment convention for the carboxyl group similar to that for the amide group, the two possible directions consistent with the observed dichroic ratio ( $f_c/f_b$ ) = 0.29 are  $-57^\circ$  and  $0^\circ$ . As far as we know, this result is the first evidence for the polarization of the carboxyl  $NV_1'$  transition. As will be discussed later, INDO/S calculations place the carboxyl  $NV_1'$  band near this energy but at an angle of  $-17^\circ$ . However, as will be seen, there are two other modest transitions predicted in this region. When all three bands are lumped together, the predicted dichroic ratio for this vicinity yields an angle of  $-52^\circ$  (or  $-4^\circ$ ). Interpretation of experimental spectra must be made with considerable caution in the face of such possible spectral congestion.

The barely perceptible foot near 57 kK along the  $b$  axis might represent the  $R_1'$  band of the carboxyl group and not, for example, a component of the peptide  $NV_1$  transition. If so, then the dichroic ratio of the amide  $NV_1$  band does in fact remain very high throughout the band. Distinguishing a  $c$  axis component for  $R_1'$  is not possible so that no suggestion regarding the polarization of the carboxyl  $R_1'$  band can be given. Finally, the  $W'$  carboxyl band is expected to occur between 46–48 kK and to have an extinction coefficient of about 30. This band is not individually distinguishable owing to its weakness and the simultaneous presence of the somewhat stronger amide  $n \rightarrow \pi^*$  ( $W$ ).

**Crystal Interactions.** *N*-Acetylglycine provides an opportunity to consider a modification of the usual exciton mixing crystal calculation, for there are two different chromophores (amide and carboxyl) located at different positions of each molecule at each unit cell site. To our knowledge such a system has not been worked through before. In what follows we assume the two chromophores of a given molecule are essentially independent so that any molecular wave function can be written as a simple product of single chromophore functions

$$\phi_{\text{amide}}^i \phi_{\text{carboxyl}}^{i'}$$

where the superscripts refer to individual electronic states of the particular chromophore. Here we will consider only singly excited functions where both  $i$  and  $i'$  cannot differ from their ground state value of zero simultaneously. Thus the  $j$ th one-site crystal function can be written as

$$\psi_{l,s,c}^j = \phi_{l,s,c}^i \prod_{\substack{l,s \\ c' \neq c}} \phi_{l,s,c'}^0$$

where  $j$  is representative of some particular excited state  $i$  of chromophore  $l$  on the molecule at molecular site  $s$  of unit cell  $c$  and is chosen to enumerate conveniently all electronic states of both chromophores.

Crystal functions are formed by imposing cyclic boundary conditions to give the usual phase-modulated Bloch functions.

$$\theta_{l,s}^j = \sum_c e^{ikr} \psi_{l,s,c}^j$$

Crystalline *N*-acetylglycine has a space group of  $P2_1/c$  with four molecules per unit cell. The positions are as follows: 1, ( $x, y, z$ );

(21) Basch, H.; Robin, M. B.; Kuebler, N. A. *J. Chem. Phys.* **1969**, *50*, 5048.



2,  $(\bar{x}, \bar{y}, \bar{z})$ ; 3,  $(\bar{x}, 0.5+y, 0.5-z)$ ; 4,  $(x, 0.5-y, 0.5+z)$ . The four  $|k\rangle = 0$  factor group functions along with their electric dipole authorizations therefore are

$${}^A_1\Phi_1^j = \frac{1}{2}[\theta_{1,1}^j + \theta_{2,1}^j + \theta_{3,1}^j + \theta_{4,1}^j] \quad (\text{forbidden})$$

$${}^A_2\Phi_1^j = \frac{1}{2}[\theta_{1,1}^j + \theta_{2,1}^j - \theta_{3,1}^j - \theta_{4,1}^j] \quad (\text{forbidden})$$

$${}^B_1\Phi_1^j = \frac{1}{2}[\theta_{1,1}^j - \theta_{2,1}^j + \theta_{3,1}^j - \theta_{4,1}^j] \quad b \text{ axis polarized}$$

$${}^B_2\Phi_1^j = \frac{1}{2}[\theta_{1,1}^j - \theta_{2,1}^j - \theta_{3,1}^j + \theta_{4,1}^j] \quad ac \text{ plane polarized}$$

States of different symmetry do not mix under the crystal Hamiltonian. To evaluate crystal energies and intensities, one must separately solve the appropriate secular equations for  $b$  axis and  $ac$  plane states. The matrix elements are

$${}^{\Gamma}\mathcal{H}_{i,j} = \langle {}^{\Gamma}\Phi_1^i | \mathcal{H} | {}^{\Gamma}\Phi_1^j \rangle + \Delta E_i \delta_{i,j}$$

where  $\mathcal{H}$  is the crystal Hamiltonian,  $\Gamma$  represents the symmetry species  $B_1$  or  $B_2$ ,  $\Delta E_i$  is the transition energy of transition  $i$ , and  $\delta_{ij}$  is the Kronecker delta. There will be 16 terms to evaluate for each matrix element. Each of these 16 terms can be approximated as a dipole-dipole lattice sum between transition dipole  $i$  located on chromophore 1 and transition dipole  $j$  located on chromophore 1'. For the case at hand with two chromophoric sites per molecule, there will be three categories of sums: I, both transitions located on the amide chromophore; II, both transitions located on the carboxyl chromophore; III, one transition located on each of the two chromophores. The Ewald-Kornfeld<sup>22</sup> evaluation procedure was used for the lattice sums used in this work and are tabulated in the Appendix.

A strategic question regarding the sums of category III arises. Should the intramolecular interaction between the dipoles representing transitions of the different chromophores of a given molecule be included? If one starts with spectroscopic parameters for the free, complete molecule in which the self-interaction has in some way already been accounted for, then such a term ought to be excluded from the lattice summation. If, on the other hand, the two chromophores are sufficiently separated in space, then it would appear to be appropriate to consider the two chromophores as independent systems. A normal crystal calculation will therefore take into account the self-interaction in the routine course of the crystal calculation. The model spectrum that is the starting point for a crystal calculation will then represent *free chromophore* characteristics as opposed to *free molecule* ones. The possibility of charge transfer transitions between amide and carboxyl is excluded in this scheme however.

Our strategy here has been to begin with a model, free-molecule spectrum derived mostly from the crystal spectra assuming the oriented gas model and to assume all transitions are polarized either in the molecular plane or normal to it. Presumed  $n\pi^*$  and  $R_1$  bands for both chromophores are added to the model. The parameters of the model (oscillator strengths, energies, and transition moment directions) are then varied in a systematic way until a reasonably close match with the observed spectra is obtained. All combinations of the possible polarizations for those transitions with bimodal ambiguities are alternately considered. The effects of the crystal field are not great. As an example, the model spectrum given in Table 4

**Table 4.** Model Spectrum for *N*-Acetylglycine<sup>a</sup>

|                   | $f^b$   | $\nu$ (kK) | $\lambda$ (nm) | $\Omega$ (deg) <sup>c</sup> | $\Delta\Omega$ (deg) <sup>d</sup> |
|-------------------|---------|------------|----------------|-----------------------------|-----------------------------------|
| W                 | 0.001   | 47         | 213            | $\perp$                     |                                   |
| (W')              | (0.001) | (48)       | (208)          | $\perp$                     |                                   |
| (R <sub>1</sub> ) | (0.01)  | (52)       | (192)          | (-55)                       |                                   |
| NV <sub>1</sub>   | 0.23    | 53.5       | 187            | -55                         | $\pm 5$                           |
| R <sub>1</sub> '  | 0.01    | 56.0       | 179            | [4 or -55]                  |                                   |
| NV <sub>1</sub> ' | 0.17    | 64.0       | 156            | [4 or -61]                  | $\pm 3$                           |
| NV <sub>2</sub>   | 0.1     | 72.0       | 139            | 10 or 61                    | $\pm 10$                          |

<sup>a</sup> Items marked with parentheses are inferred and not directly observed. <sup>b</sup> Oscillator strengths are three-dimensional (random) values. <sup>c</sup> Angles appearing in square brackets refer to the carboxyl convention. Others refer to the amide reference axis. <sup>d</sup> Estimated angular uncertainties from experimental resolutions.

leads to crystal spectra that closely match those from experiment. Table 5 compares the output of the assumed model both before and after crystal interactions are treated with the experimental spectra. Other combinations of possible polarizations for the carboxyl NV<sub>1</sub>' and amide NV<sub>2</sub> bands lead to very similar results. In fact, the variations are within the original experimental uncertainties.

The calculations indicate strong mixing between the amide NV<sub>1</sub> and R<sub>1</sub> bands along both the  $b$  and  $c$  axes. The resulting crystal functions are made up with roughly 50% of each. In fact the  $c$  axis components of the NV<sub>1</sub> and R<sub>1</sub> bands are calculated to be separated by 600  $\text{cm}^{-1}$  and thus would not be distinguishable. Although there is no direct evidence for the amide R<sub>1</sub> band in the spectra, the calculations support the notion that such direct evidence not only is not to be expected but in fact cannot be observed. Therefore, the lack of any direct evidence for the amide R<sub>1</sub> band of *N*-acetylglycine does not lessen the argument for its occurrence based on the propanamide work.

The occurrence of the weak "foot" at 56 kK of the  $b$  axis spectrum is the only evidence for the R<sub>1</sub>' carboxyl band. This vague feature cannot arise from a Davydov shifted component of the amide NV<sub>1</sub> transition because the crystal calculations clearly indicate such a shift is about 1000  $\text{cm}^{-1}$  to the red of the free molecule energy and not 3000  $\text{cm}^{-1}$  to the blue. Nevertheless, the observation and assignment of this band must be considered tentative. It can be noted that INDO/S calculations predict a charge transfer band ( $n \rightarrow \pi_3^*$ ) in this vicinity, but the predicted polarization is contrary to the observed feature.

Finally, additional spectra were recorded from a natural (010) face and from a face cut perpendicular to the (100) face. The latter face was prepared using an ultramicrotome technique.<sup>23</sup> Both of these faces display the molecular planes edge on, so that the spectrum polarized normal to the molecular planes was recorded. The reflectivity spectrum in each case was nearly flat and showed no features that could be attributed to either the  $n \rightarrow \pi^*$  bands or possibly other more intense, perpendicularly polarized bands.

**Summary.** The spectrum of *N*-acetylglycine is made up of at least seven transitions (some inferred). Table 4 summarizes the results presented so far. Estimated uncertainties are based on reasonable latitude in resolving crystal spectra, the variation of dichroic ratios with transition moment directions, *etc.*

### SCF Molecular Orbital Calculations

We have performed INDO/S calculations on both propanamide and *N*-acetylglycine. Since chromophores of low symmetry such as amide and carboxyl exhibit transitions with variable inplane transition moment directions, experimental

Table 5. Crystal Spectra of (100) Face of *N*-Acetylglycine<sup>a</sup>

|                   | <i>b</i> axis             |                   |           | <i>c</i> axis             |                   |             |
|-------------------|---------------------------|-------------------|-----------|---------------------------|-------------------|-------------|
|                   | oriented gas <sup>c</sup> | calc <sup>c</sup> | observed  | oriented gas <sup>c</sup> | calc <sup>c</sup> | observed    |
| W                 | 0.000 (48.0)              | 0.000 (48.0)      | ... (>46) | 0.000 (48.0)              | 0.000 (48.0)      | ... (>46)   |
| W'                | 0.000 (48.5)              | 0.000 (48.5)      | ... (>46) | 0.000 (48.5)              | 0.000 (48.5)      | ... (>46)   |
| R <sub>1</sub>    | 0.000 (52.0)              | 0.000 (51.8)      | ... (...) | 0.030 (52.0)              | 0.42 (51.7)       | 0.72 (52.0) |
| NV <sub>1</sub>   | 0.000 (53.5)              | 0.000 (52.4)      | ... (...) | 0.69 (53.5)               | 0.31 (52.3)       |             |
| R <sub>1</sub> '  | 0.029 (56.0)              | 0.032 (56.0)      | 0.03 (56) | 0.007 (56.0)              | 0.004 (56.0)      | 0.11 (64.0) |
| NV <sub>1</sub> ' | 0.36 (64.0)               | 0.37 (63.7)       | 0.37 (64) | 0.15 (64.0)               | 0.11 (63.5)       |             |
| NV <sub>2</sub>   | 0.24 (72.0)               | 0.22 (71.7)       | 0.2 (72)  | 0.06 (72.0)               | 0.06 (72.6)       | ~0.05 (72)  |

<sup>a</sup> One-dimensional oscillator strengths and energies (in kiloKaisers) in parentheses. <sup>c</sup> Calculated from the model spectrum of Table 4 with the first choice of angles given there.

polarization directions provide additional targets with which to tune the calculational apparatus. Volosov<sup>24</sup> has previously reported calculations of the electronic transitions of myristamide, *N,N'*-diacetylhexamethylenediamine, and *N*-acetylglycine using a special version of CNDO called CNDO/OPTIC.

The calculations here employed the standard parameter set suggested by Ridley and Zerner,<sup>25</sup> and no attempt has been made to "tune" the parameterization. Only singly excited configurations were used. For propanamide the highest 14 filled orbitals and the lowest 12 empty orbitals were included giving 168 excited configurations overall in the CI calculations. For *N*-acetylglycine the highest 14 filled and lowest 14 unfilled orbitals were used giving 196 excited configurations in all. In what follows, the results of both INDO/S calculations together with Volosov's CNDO/OPTIC results will be contrasted and compared with the experimental results presented earlier.

**Propanamide.** The positions of the hydrogen atoms given in the crystal structure paper are for various reasons somewhat uncertain,<sup>13</sup> and for our purpose the hydrogen atoms have been positioned in a symmetrical way about the framework atoms so as to maintain planar symmetry. The results of the calculations fulfill all expectations based on general MO ideas. All predicted transitions to at least 85 kK can be described as arising mainly from single configurations derived from electron transition between MOs 12 through 15 (HOMO) and 16 (LUMO) to 18.

The *n* orbital is strongly localized on the oxygen atom (~80%) and provides the lowest energy transition (*n* →  $\pi_3^*$ ) of the spectrum. This is the W band. The calculated position of 32 kK (310 nm) is 14 kK to the red of its observed position (46 kK). This difficulty with *n* →  $\pi^*$  energies has been a persistent problem in such calculations. The NV<sub>1</sub> band ( $\pi_2$  →  $\pi_3^*$ ) is calculated to appear at 53.4 kK (187 nm) with *f* = 0.31. The  $\pi_2$  orbital is mainly the antisymmetric combination of the 2*p* $\pi$  orbitals of the oxygen and nitrogen atoms, whereas the  $\pi_3^*$  orbital is dominantly the 2*p* $\pi$  orbital of the central carbon of the amide group. Although the calculated oscillator strength of *f* = 0.31 is somewhat high compared with the experimental value (*f* = 0.17), the computed transition moment direction (-28°) is near the experimental value (-35°). There are two transitions (*n* →  $\sigma_2^*$  and  $\pi_2$  →  $\sigma_2^*$ ) predicted in the region between 60 and 68 kK, but these transitions are probably too weak to observe. The experimental curves display a broad absorption region in the 75–80 kK region, and the observed dichroic ratio (*b/c*) for this region is about 1.8. These intensities are consistent with an in-plane polarized transition of *f* ≈ 0.1 at  $\Omega$  = -71° or +46°. In fact, the calculation gives as the second most prominent transition the  $\pi_1$  →  $\pi_3^*$  (or NV<sub>2</sub>) at 71 kK with *f* = 0.22 and  $\Omega$  = +49°. Presumably the positive choice from the crystal spectra is therefore preferred. This is the band also called the amide Q band.

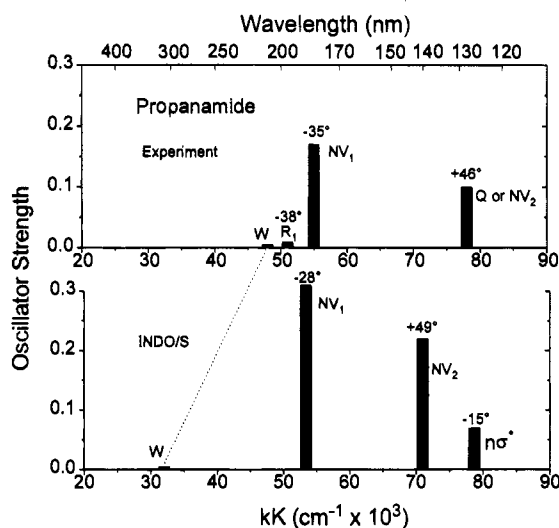


Figure 12. Comparison of the experimental model propanamide spectrum (upper) with that obtained with INDO/S calculations (lower).

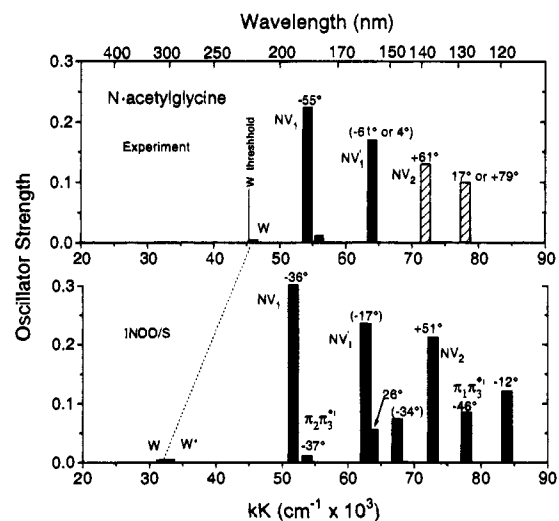


Figure 13. Comparison of experimental model *N*-acetylglycine spectrum (upper) with that predicted with INDO/S calculations (lower). Assignment of the cross-hatched transitions are relatively more uncertain than those shown as solid bars. The calculated transitions that are not otherwise identified are all either *n* $\sigma^*$  or *n'* $\sigma^*$  transitions.

The model spectrum derived from the crystal spectra is schematically compared with the calculated results in Figure 12. With the exception of the position of the W band, the overall agreement between the electronic structure calculations and experiment is excellent. Since the amide R<sub>1</sub> band does not appear in the calculated results, the argument that it is of Rydberg origin is strengthened. Even though Robin has argued that such Rydberg transitions are not to be observed in condensed phases,<sup>3,4</sup> we feel that such a transition most likely

(23) Xu, S.; Clark, L. B. *J. Am. Chem. Soc.* **1994**, *116*, 9227.

(24) Volosov, A. *J. Chem. Phys.* **1987**, *87*, 6653.

does not vanish entirely. Rather, it may be significantly distorted so that its original nature becomes unrecognizable. Surely some vestige must remain, and given the proper mixing conditions it may blossom into an observable transition even in condensed phases. The  $n \rightarrow R$  assignment with R representing 3s orbitals in the amide group would have a natural in-plane polarization direction approaching  $\pm 90^\circ$ . The value of  $\sim -55^\circ$  used in the crystal mixing calculations is not in conflict with these ideas.

The results presented by Volosov<sup>24</sup> for myristamide (and *N,N'*-diacetylhexamethylenediamine) using the CNDO/OPTIC method are in reasonable agreement with the present calculations for the W band (33 kK,  $f = 0.007$ ) and the  $NV_1$  transition (58 kK,  $f = 0.12$ ,  $\Omega = -27^\circ$ ). However, his method does not produce the  $NV_2$  transition in the vicinity; rather it places a very strong transition ( $n\sigma^*$ ,  $f = 0.48$ ) at 78 kK polarized at  $73^\circ$ . Such a transition is not observed in the crystal spectra.

***N*-Acetylglycine.** Conventional wisdom would hold that the amide and carboxyl groups ought to be semi-independent and that the spectrum of *N*-acetylglycine should approximately be the superposition of the two individual chromophoric spectra with the addition of some weak charge transfer bands. As we shall see, the calculations yield results in accord with these ideas.

*N*-Acetylglycine is almost planar in the crystal, and this structure was used in the calculations. For the most part, configuration mixing does not change the qualitative correctness of the simple orbital assignment of transitions. Three relatively strong bands are predicted at the energies where relatively strong bands are observed. The amide  $NV_1$  ( $\pi_2 \rightarrow \pi_3^*$ ) is calculated to occur at 51.7 kK,  $f = 0.30$ , and  $\Omega = -36^\circ$ . These values compare reasonably with the experimental values of 52 kK (193 nm),  $f = 0.24$  and  $\Omega = -55^\circ$ . The second principal band at 62.7 kK (159 nm),  $f = 0.24$ , is the  $NV_1'$  transition of the carboxyl group and is predicted at an in-plane direction of  $-17^\circ$  (carboxyl origin). The position and intensity are in reasonable agreement with the experimental spectra, but the two possible experimental directions are  $-57^\circ$  and  $+1^\circ$ . Either way, the differences amount to substantial angular swings. As mentioned earlier, if the three predicted transitions between 63 and 67 kK are lumped together, then the apparent polarizations of the combined result are  $-52^\circ$  and  $-4^\circ$ . Probably such situations cannot be avoided. Finally, the third strong band is the amide  $NV_2$  ( $\pi_1 \rightarrow \pi_3^*$ ) predicted at 72.8 kK,  $f = 0.21$ ,  $\Omega = +51^\circ$ . Experimentally, a band is observed in the 72–75 kK region that, if derived from the amide group, has approximate polarization direction possibilities of  $+60^\circ$  or  $+10^\circ$  (both  $\pm 10^\circ$ ).

As with propanamide the  $n \rightarrow \pi^*$  transitions are predicted to occur far to the red ( $>10$  kK) of their actual positions. The calculations give the amide  $n \rightarrow \pi_3^*$  (W) at 31 kK and the carboxyl  $n' \rightarrow \pi_3^*$  (W') at 32 kK; whereas the lowest possible experimental position is about 46 kK. Again, as seen with propanamide, the energies of  $n \rightarrow \pi^*$  transitions are notoriously in error.

It is of interest to examine the cross-talk (or charge transfer) transitions predicted by theory. The lowest such transition is between the  $\pi_2$  amide orbital and the  $\pi_3^*$  carboxyl orbital and is predicted to be fairly weak ( $f = 0.01$ ). This transition is predicted to occur at 54 kK and to have an in-plane polarization ( $-37^\circ$ ) almost identical to that of the strong amide  $NV_1$  band at 52 kK. Thus the  $\pi_2 \rightarrow \pi_3^*$  band will be completely obscured and therefore not separately observable in the crystal spectra. It is not the origin of the "foot" observed in *b* polarization at 56 kK. Finally, we mention that what we have labeled as the amide  $\pi_1$  orbital is different from the other orbitals in that it is distributed across the entire molecule to a much greater extent

than the other molecular orbitals. Consequently, the transition strength for  $\pi_1 \rightarrow \pi_3^*$  is enhanced.

Volosov's CNDO/OPTIC results are comparable with the results obtained here except that his calculation predicts a strong perpendicularly polarized  $\pi\sigma^*$  near 70 kK. The spectra taken from the crystal face cut normal to the planes of the molecules show that no such band occurs in the spectrum. Finally, his calculation predicts the carboxyl  $NV_1'$  band to be polarized at  $-27^\circ$ , and this value compares with the INDO/S result of  $-17^\circ$ . Neither are very close to the experimental possibilities of  $-57^\circ$  or  $+1^\circ$  although the piling up of transitions here may account for the disparity. A number of other electronic structure calculations on various amides have been carried out over the years.<sup>4,26–28</sup> We note here the *ab initio* study by Matos and Roos on formamide.<sup>28</sup> Only the  ${}^1,3n\pi_3^*$  and  ${}^1,3\pi_2\pi_3^*$  transitions were given for various SCF calculations. The  $NV_1$  polarization direction was computed to be about  $-38^\circ$  with an oscillator strength of between 0.25 and 0.45 depending on the calculation. Even if alkyl substitution on the nitrogen swings the angle  $-5^\circ$  to  $-10^\circ$  or so, the overall agreement is very good in our estimation.

## Conclusion

There is general agreement between the spectra of both propanamide and *N*-acetylglycine and the predictions of the INDO/S theory. The agreement extends beyond transition energies and oscillator strengths to include general transition moment directions.

An amide group as represented by the propanamide spectrum is dominated by the two  $\pi\pi^*$  valence shell transitions ( $NV_1$  and  $NV_2$ ). The presence of the low energy, weak  $n \rightarrow \pi^*$  band (W) is certain, and it is expected to appear with substantially mixed polarization. Evidence is presented for the  $R_1$  band as appearing between the W and  $NV_1$  bands and as being inherently weak ( $f \approx 0.01$ ). It is polarized not far from that of the nearby  $NV_1$  band although appreciable crystal field mixing of  $R_1$  and  $NV_1$  obscure the natural characteristics of the  $R_1$  transition. There is little absorption intensity between  $NV_1$  and what is presumably the second  $\pi\pi^*$  band ( $NV_2$ ,  $f \approx 0.1$ ) at 78 kK.  $NV_1$  and  $NV_2$  display polarization directions of  $-36^\circ$  and  $+46^\circ$ . The latter value was picked over the alternative possibility of  $-72^\circ$  by correspondence with the INDO/S calculations.

The spectra taken of *N*-acetylglycine show a superposition of both a secondary amide (peptide) group and a carboxyl group. The spectra can be reasonably interpreted as arising from the amide transitions W,  $NV_1$ ,  $NV_2$  and the carboxyl transitions W',  $R_1$ ,  $NV_1'$ . No direct evidence for the  $R_1$  band is observed, and even the evidence from the  $R_1'$  band is marginal. The important peptide  $NV_1$  transition moment direction is in the range  $-51^\circ$  to  $-60^\circ$ . This band is significantly red-shifted relative to its position in propanamide, and this shift precludes finding evidence for the now overlapped amide  $R_1$  transition. The  $NV_2$  amide band is observed near 75 kK at a direction near  $46^\circ$ .

Tentative evidence is found for the  $R_1'$  band of the carboxyl group near 57 kK. However, a strong carboxyl transition at 64 kK with possible polarizations of  $-57^\circ$  or  $1^\circ$  is definitely present. The INDO/S calculations predict this transition at  $-17^\circ$  and offer no clear choice in resolving the crystal ambiguity.

The INDO/S calculations with the standard parameterization provide a reasonable description of the electronic spectra. As

(25) Ridley, J.; Zerner, M. C. *Theor. Chim. Acta* **1973**, *32*, 111.

(26) Volosov, A. P.; Zubkov, V. A.; Birshtein, T. M. *Tetrahedron* **1975**, *31*, 1259.

(27) Volosov, A. *Int. J. Quant. Chem.* **1988**, *34*, 471.

(28) Matos, J. M. O.; Roos, B. O. *J. Am. Chem. Soc.* **1988**, *110*, 7664.

usual  $n \rightarrow \pi^*$  transition energies are far too low, but the energies, oscillator strengths, and transition moment directions of the other principal bands seem adequately accounted for.

The shift to somewhat lower energy ( $\sim 2$  kK) of the amide  $NV_1$  band upon going from a primary to a secondary amide appears to be derived from the alkyl substitution at nitrogen. INDO/S calculations on acetamide, *N*-methylacetamide, and *N*-dimethylacetamide predict an increasing red shift relative to acetamide for  $NV_1$ . Further the directional shift of  $-20^\circ$  for  $NV_1$  going from propanamide to *N*-acetylglucine is representative of a change from a primary to a secondary amide. INDO/S calculations give a directional shift for  $NV_1$  of  $-9^\circ$  going from acetamide to *N*-methylacetamide and a similar shift of  $-8^\circ$  between propanamide and *N*-acetylglucine. Woody<sup>2</sup> reported CNDO/S calculations on acetamide and *N*-methylacetamide as part of a study dealing with the effects of the permanent electric dipole field in crystals. Predicted gas phase energies were reported, but transition moment direction results were not explicitly stated.

The amide portion of the *N*-acetylglucine spectrum is the prototype for the peptide chromophore, and the results derived from the *N*-acetylglucine crystal spectra should be the spectral model used for calculations of optical properties of polypeptides, etc. The difference between the  $NV_1$  polarization direction universally used in the past ( $-41^\circ$  for myristamide) and the *N*-acetylglucine value of  $-55^\circ$  is significant.

**Acknowledgment.** We thank the National Institutes of Health for support of this work through Grant No. R01 GM38575. Dr. Blair Campbell is thanked for his contribution in the early phase of this work. Dr. Shimin Xu is thanked for his assistance with the INDO/S calculations.

## Appendix

**Crystal Structure of *N,N'*-Diacetylhexanediamine.** As mentioned in the text, errors in the atomic coordinates for the structure reported by Bailey<sup>29</sup> in 1955 have been found. The errors were discovered when projections onto various crystal faces showed distortions. No corrections were found in the literature, but it was discovered that the Cambridge Structural Database had been updated with consistent coordinates. The correct coordinates are given in Table 6. All negative signs had been omitted in the original publication. A projection of the unit cell onto (100) is given in Figure 14. The actual projection of the amide  $NV_1$  transition moment (shown in the figure as open arrows) is not consistent with the analysis given by Peterson and Simpson.<sup>8</sup> The face they examined must have been other than (100), or else the axes were misidentified.

**Table 6.** Fractional Atom Coordinates for *N,N'*-Diacetylhexanediamine<sup>a</sup>

|     | <i>a</i> | <i>b</i> | <i>c</i> |
|-----|----------|----------|----------|
| C1  | 0.0338   | -0.033   | 0.114    |
| C2  | 0.1178   | -0.220   | -0.024   |
| C3  | 0.1872   | -0.283   | 0.210    |
| C4  | 0.3208   | -0.583   | 0.230    |
| C5  | 0.4032   | -0.763   | 0.073    |
| N6  | 0.2654   | -0.463   | 0.075    |
| O7  | 0.3097   | -0.550   | 0.485    |
| H8  | 0.079    | -0.152   | 0.303    |
| H9  | 0.980    | -0.855   | 0.190    |
| H10 | 0.171    | -0.897   | 0.822    |
| H11 | 0.072    | -0.600   | 0.709    |
| H12 | 0.234    | -0.901   | 0.401    |
| H13 | 0.134    | -0.604   | 0.288    |
| H14 | 0.282    | -0.506   | 0.866    |

<sup>a</sup> Only one-half of the molecule is given. The remaining atoms can be found by inverting the positions given through the origin.

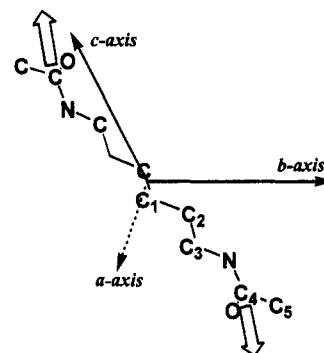


**Figure 14.** Projection of the one molecule of the unit cell of *N,N'*-diacetylhexanediamine onto the *bc* face. The direction of the amide  $NV_1$  transition is shown as the open arrows. This system is triclinic, and the dotted *a* axis shown represents the projection of this axis onto the (100) face.

**Table 7.** Dipole-Dipole Lattice Sums ( $\text{cm}^{-1}/\text{\AA}^2$ ) for Simple Amides

|                          | <i>a,a</i> | <i>b,b</i> | <i>c,c</i> | <i>a,b</i> | <i>a,c</i> | <i>b,c</i> |
|--------------------------|------------|------------|------------|------------|------------|------------|
| Propanamide <sup>a</sup> |            |            |            |            |            |            |
| 1,1                      | -350       | -2954      | -84        | 0          | 157        | 0          |
| 1,2                      | -5321      | -2549      | 1708       | 522        | 1349       | -206       |
| 1,3                      | -94        | -475       | -1664      | 0          | -602       | 0          |
| 1,4                      | -172       | -492       | -4572      | 0          | 1896       | 0          |
| Myristamide <sup>b</sup> |            |            |            |            |            |            |
| 1,1                      | 170        | -3162      | 2026       | 0          | -15        | 0          |
| 1,2                      | 2026       | -2402      | -189       | 466        | -2203      | 1046       |
| 1,3                      | -1845      | -345       | 1043       | 0          | 1122       | 0          |
| 1,4                      | -4709      | 401        | 3293       | 0          | 424        | 0          |

<sup>a</sup> Sites 1-4 are (*x,y,z*), ( $\bar{x},\bar{y},\bar{z}$ ), ( $\bar{x},1/2+y,1/2-z$ ), ( $x,1/2-y,1/2+z$ ).  
<sup>b</sup> Sites 1-4 are (*x,y,z*), ( $\bar{x},\bar{y},\bar{z}$ ), ( $1/2-x,1/2+y,\bar{z}$ ), ( $x+1/2,1/2-y,z$ ).

**Table 8.** Dipole-Dipole Inner Lattice Sums ( $\text{cm}^{-1}/\text{\AA}^2$ ) for *N*-Acetylglucine<sup>a</sup>

|                   | <i>a,a</i> | <i>b,b</i> | <i>c,c</i> | <i>a,b</i> | <i>a,c</i> | <i>b,c</i> |
|-------------------|------------|------------|------------|------------|------------|------------|
| Amide-Amide       |            |            |            |            |            |            |
| 1,1               | -4865      | 1395       | -2363      | 0          | 3635       | 0          |
| 1,2               | 105        | 103        | -1240      | 21         | -61        | 373        |
| 1,3               | 52         | -3694      | 452        | 0          | -36        | 0          |
| 1,4               | 52         | -668       | -925       | 0          | -8         | 0          |
| Carboxyl-Carboxyl |            |            |            |            |            |            |
| 1,1               | -4865      | 1395       | -2363      | 0          | 3635       | 0          |
| 1,2               | 125        | -3941      | 572        | 37         | -91        | -120       |
| 1,3               | 11         | -1779      | -399       | 0          | -4         | 0          |
| 1,4               | 187        | 2063       | -2272      | 0          | -5         | 0          |
| Amide-Carboxyl    |            |            |            |            |            |            |
| 1,1               | -2941      | 2927       | -2464      | -184       | 1961       | -1968      |
| 1,2               | -323       | -2558      | -122       | -65        | 264        | 1055       |
| 1,3               | -44        | -2216      | -169       | -55        | 8          | -460       |
| 1,4               | -1180      | 374        | -730       | 610        | 377        | 1709       |

<sup>a</sup> Sites 1-4 are (*x,y,z*), ( $\bar{x},\bar{y},\bar{z}$ ), ( $\bar{x},1/2+y,1/2-z$ ), ( $x,1/2-y,1/2+z$ ).

**Index of Refraction of LiF.** Values of *n* for LiF at about 20 °C have been collected by Palik and Hunter.<sup>30</sup>

The form  $n = a + bx + cx^2 + dx^3 + ex^4$  was fit to these data using a least squares routine where  $x = (\text{wavelength in nm})^{-1}$ . The coefficients found are as follows:  $a = 1.395$ ,  $b = -14.06$ ,  $c = 9.412 \times 10^3$ ,  $d = -1.642 \times 10^6$ ,  $e = 1.355 \times 10^8$ .

**Dipole-Dipole Lattice Sums.** All lattice sums were evaluated with the Ewald-Kornfeld procedure.<sup>22</sup> In this procedure the full lattice sum ( $T_{ij}$ ) is broken into an inner part ( $t_{ij}$ ) and a

(29) Bailey, M. *Acta Crystallogr.* **1955**, *8*, 575.

(30) Palik, E. D.; Hunter, W. R. *Handbook of Optical Constants of Solids*; Academic Press: Inc.: New York, 1985; pp 675-693.

macroscopic or long-range part

$$T_{ij} = d_i d_j t_{ij} + \frac{4\pi}{V_0} (\mathbf{d}_i \cdot \mathbf{k})(\mathbf{d}_j \cdot \mathbf{k})$$

where  $\mathbf{k}$  is the exciton wave vector (normal to the particular crystal face under consideration), the  $d$ 's are transition moment vectors, and  $V_0$  is the volume of the unit cell. The inner part,  $t_{ij}$ , for the various unit vectors along the crystallographic axes are given in Tables 7 and 8. The macroscopic term must be

added to complete any given sum. The dipole centers were taken at the central carbon atom of the amide or carboxyl group in all cases. In addition, the values for individual site combinations are as follows: (1,1=2,2=3,3=4,4), (1,2=2,1=3,4=4,3), (1,3=2,4=3,1=4,2) and (1,4=2,3=3,2=4,1). The sums given here are for various combinations of unit vectors along the unit cell axes. Any general dipole-dipole lattice sum can be evaluated from the numbers given.

JA950829R